

RESEARCH

Open Access



Mechanisms of HRAS regulation of liver hepatocellular carcinoma for prognosis prediction

Xingbao Fang^{1†}, Yan Cai^{2†}, Zhuoyu Zhao¹, Shaohua Yang¹, Zhaojun Li¹, Xiongbing Peng¹, Meifang Hang¹, Peiwan Liu^{1*} and Yuehong Li^{1*}

Abstract

Background Liver hepatocellular carcinoma (LIHC) often has a poor prognosis. Since the relationship between HRas proto-oncogene, GTPase (HRAS) and LIHC has not been elucidated, the aim of this study was to explore the mechanisms by which HRAS is involved in regulating the prognosis of LIHC.

Methods We used The Cancer Genome Atlas (TCGA) database to characterize differences in HRAS gene expression between LIHC patients and healthy individuals. In addition, we analysed the relationships between HRAS gene expression levels and the clinicopathological characteristics of LIHC patients. Next, we used univariate and multivariate Cox regression analyses to identify prognostic factors. Differentially expressed genes were identified between the low- and high-expression groups, and KEGG and GO analyses and GSEA were performed to study the underlying mechanisms. The effects of high and low HRAS expression on the prognosis of LIHC patients was determined according to CIBERSORT. We subsequently assayed HRAS gene expression at the cellular level, and these data were validated in a tumour xenograft model.

Results We established and validated the HRAS gene as a prognostic signature and analysed the relationships between HRAS expression levels and clinicopathological features. Patients were categorized into high and low HRAS gene expression groups. We determined that high HRAS expression is associated with carbon metabolism, the PPAR signalling pathway, and small molecule catabolism in cancer. Furthermore, we conclude that the poor prognosis that results from elevated HRAS expression is associated with immune cell infiltration. We used LASSO + KNN to build an AI classification model that shows good performance in distinguishing liver cancer tissues from normal tissues. Finally, we verified that HRAS is highly expressed in hepatocellular carcinoma cells and promotes tumour growth.

Conclusion We identified and validated the role of HRAS in hepatocellular carcinoma to assess hepatocellular carcinoma prognosis. The results of this study can be applied to predict survival, for personalized liver cancer treatment strategies, and provide information for the development of potential targeted therapies and new ideas for liver cancer patient treatment.

Keywords Liver hepatocellular carcinoma, HRAS, Survival prediction, Prognostic mechanisms

[†]Xingbao Fang and Yan Cai contributed equally to this work.

*Correspondence:

Peiwan Liu
liupeiw@kmmu.edu.cn
Yuehong Li
liyuehong@kmmu.edu.cn

Full list of author information is available at the end of the article



Introduction

Liver hepatocellular carcinoma (LIHC) is the most common cause of cancer-related deaths worldwide, with the number of cases expected to exceed 1 million by 2025 [1]. Its incidence is increasing every year and is higher in developing countries [2]. Although organ transplantation, surgical resection, and anticancer drugs are the mainstays of treatment for LIHC, no proven treatment has been found due to the lack of donor livers and tumour heterogeneity [3]. Therefore, exploring the mechanisms of LIHC development is essential for prognostic modelling.

HRas proto-oncogene GTPase (HRAS) is a member of the RAS family and one of the most heavily mutated genes in human cancers [4]. The HRAS gene has been shown to be associated with advanced cancer tumour staging and metastasis [5]. Moreover, GINS complex subunit 1 (GINS1), which is involved in tumour development under pathological conditions, induces liver cancer stem cells by activating the HRAS pathway to promote the development of LIHC [6]. Chen et al. [7] reported that HRAS upregulation was associated with both the development of LIHC and its poor prognosis. In summary, controlling the development of HRAS would be beneficial to improving LIHC prognosis.

Recent studies have shown that the tumour microenvironment plays an important role in the development of tumours [8]. Additionally, immune cells in the immune microenvironment influence LIHC prognosis. Dendritic cells from LIHC patients have an impaired ability to trigger an immune response while promoting immunosuppression [9]. In addition, T-cell surface cell markers can indicate cancer prognosis [10]. Therefore, we sought to generate a model to predict LIHC prognosis by combining data regarding the immune response and HRAS gene expression.

In this study, we analysed HRAS gene expression data in LIHC tissues and healthy tissues obtained from the TCGA database, analysed the relationships between patient HRAS expression levels and clinicopathological characteristics, and explored the relationships between HRAS gene expression and cancer prognosis. The correlation between the expression of the HRAS gene and other genes in the high-expression group was examined, and the 10 genes with the highest correlation were selected. CIBERSORT analysis was used to investigate the mechanism by which elevated HRAS expression leads to poor prognosis in LIHC. Finally, we validated the overexpression of HRAS in hepatocellular carcinoma cells and revealed that it promotes tumour growth, thus affecting cancer prognosis.

Materials and methods

Data collection and preprocessing

Advances in high-throughput sequencing analyses across multiple cancer types, coupled with the evolution of bioinformatics methods, have facilitated the discovery of key targets and new predictive features [11]. The online data mining platform and cancer microarray database ONCOMINE (<https://www.oncomine.com/>) was used to analyse the transcription levels of HRAS genes among different cancers. Information regarding the gene expression profiles and pertinent clinical information, including data from 371 LIHC patients and 50 healthy individuals, was acquired from The Cancer Genome Atlas (TCGA). The datasets GSE76427 (115 LIHC patients and 52 healthy patients), GSE64041 (60 LIHC patients and 60 healthy patients), and GSE25097 (268 LIHC patients and 243 healthy patients) were used for external validation.

Analysing the correlation between HRAS expression and prognosis

The relationships between HRAS gene expression levels and the clinicopathological characteristics of the patients in the TCGA database were analysed. Additionally, the relationships between HRAS gene expression and sex, age, pathological stage, N or M stage, and prognosis were investigated. Univariate and multivariate Cox regression analyses were used to determine whether HRAS was an independent prognostic factor for OS in patients with LIHC.

Functional annotation and enrichment analysis

The samples with HRAS gene expression below the mean expression level were combined in the HRAS low-expression group and the other samples were combined in the HRAS high-expression group; then, analysis of variance was performed. Kyoto Encyclopedia of Genes and Genomes (KEGG) and Gene Ontology (GO) enrichment analyses and gene set enrichment analysis (GSEA) were conducted to calculate the correlations between the expression levels of the HRAS gene and the other genes in the high-expression group.

Prognostic model of LIHC

The 10 other genes in the high-expression group with the highest correlation with the HRAS gene were selected and used to construct a PPI network. The PPI network was evaluated using the CytoHubba plug-in in Cytoscape, and 10 hub genes were selected from among them. Kaplan–Meier survival curve analysis was performed on these 20 genes to identify genes associated with poor

LIHC prognosis, and these genes were included with the HRAS gene for prognostic modelling.

Tumour immune cell infiltration analysis

To further analyse the correlation between the expression level of HRAS and the extent of immune cell infiltration in LIHC tumours, the relationships among HRAS expression and the abundance of different infiltrating immune cells were analysed using the CIBERSORT algorithm. The mechanisms of poor LIHC prognosis were investigated by examining high or low HRAS expression levels that strongly affect immune cell infiltration.

The steps of bioinformatics analysis are presented in Fig. 1.

Cell culture and reagents

The human hepatocellular carcinoma cell lines HepG2, HepB3, HuH-7 and HL-7702 were purchased from the Shanghai Cell Institute. These cells were cultured in 1640 culture medium supplemented with 10% heat-inactivated foetal bovine serum (Wisent, 086–150) and penicillin/streptomycin and were incubated at 37 °C in a humidified atmosphere with 5% CO₂. HRAS was subsequently knocked down in these to further investigate the effect of this gene on LIHC.

The anti-HRAS antibody was obtained from Beyotime (A0216).

Hep3B cells and Huh-7 cells were subjected to HRAS knockdown and then cocultured with CD4 +T cells to detect the surface markers of immune cells.

Western blot analysis

For immunoblot analysis, the cells were harvested and lysed in RIPA lysis buffer (Solarbio, R0010). Protein concentrations were determined using a BCA protein assay kit (Beyotime, P0010). Protein samples (20 mg per lane) were separated via 8–15% SDS–polyacrylamide gel electrophoresis and transferred to polyvinylidene difluoride membranes (Millipore, ISEQ00010). The membranes were subsequently blocked in 5% nonfat milk (BD, 232100) in phosphate-buffered saline (PBS) supplemented with 0.1% Tween- 20 and probed with primary antibodies overnight at 4 °C. The secondary antibody was diluted 1:5000 with TBST, added to the cells for 2 h of incubation at room temperature, and then the cells were washed three times with TBST on a decolorizing shaker at room temperature, followed by chemiluminescence detection with Tanon ECL. ImageJ software was used to calculate the expression level of each protein, which was normalized to that of GAPDH.

qRT–PCR

Total RNA was extracted using RNAiso Plus (Invitrogen) for 5 min at room temperature, and then the cells were centrifuged at 12,000 ×g for 15 min at 4 °C to obtain the

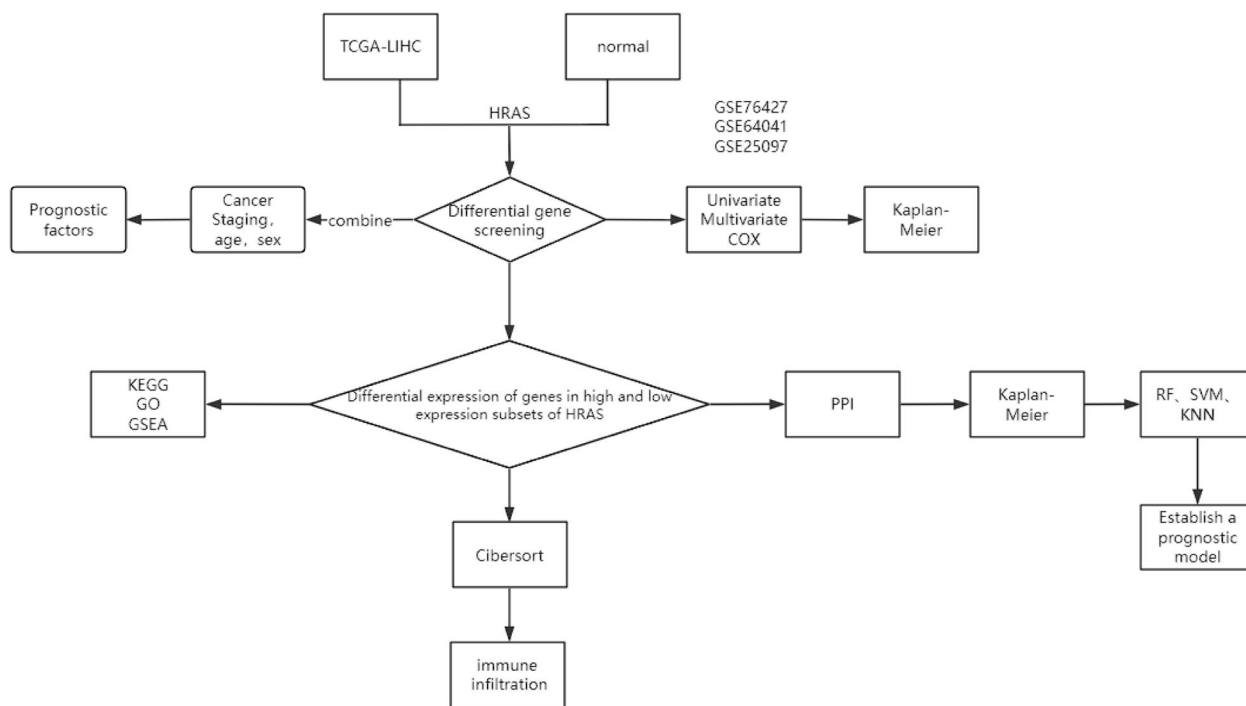


Fig. 1 Flowchart of the bioinformatics analysis

supernatant. The supernatant was then added to isopropanol, mixed well, and centrifuged at $7500 \times g$ for 10 min at 4 °C. After precipitation with DEPC aqueous solution, the RNA was solubilized, and the RNA concentration (in ng/ μ l) was determined using UV absorbance measurements. Quantitative real-time PCR (qPCR) was used to measure mRNA expression using the PrimeScript RT Kit (TaKaRa, RR047) and SYBR Premix Ex Taq (TaKaRa) according to the manufacturer's instructions. GAPDH was used as an internal control.

Primers used in this study (Sangon):

hsa-HRAS-F: ATGACGGAATATAAGCTGGTGGT
 hsa-HRAS-R: GGCACGTCTCCCCATCAATG
 hsa-GAPDH-F: GGAGCGAGATCCCTCCAAAAT
 hsa-GAPDH-R: GGCTGTTGTCATACTTCT
 CATGG

In vivo xenograft mouse model

All animals were purchased from GemPharmatech Co., Ltd, which license number is SYXK(SU) 2023–0029.

Four- to six-week-old BALB/c nude mice were housed and maintained in the SPF-level animal laboratory. All animal experiments were carried out in accordance with the National Institutes of Health Guide (Guide for the Care and Use of Laboratory Animals, 2011) and approved by the Animal Experimental Ethics Committee of The First People's Hospital of Qujing City, Yunnan Province (no. Kmmu20221137).

The nude mice were randomly divided into 2 groups of 6 after 1 week of acclimatization and inoculated with tumour cells in the axillae of the forelimbs, and after tumour nodules had formed (approximately 2 weeks), the tumour size was measured twice a week. The nude mice were observed for 4 weeks, after which they were sacrificed via CO₂ inhalation and the tumour tissues were removed.

Immunohistochemical evaluation of HRAS expression in mouse tumour tissues

The tumour tissues were sectioned and incubated with primary and secondary antibodies, after which DAB solution was added. Colour development was subsequently observed under a microscope.

Medium-to-representative HRAS staining images in cancerous and near-normal tissues were detected by immunohistochemistry.

Haematoxylin–eosin staining

After sectioning, the tumour tissues were stained with haematoxylin–eosin before observation.

Immunofluorescence evaluation of HRAS expression in mouse tumour tissues

After sectioning, Triton X-100 was added to the tumour tissue for 10 min of permeabilization. Then, the samples were washed with PBS, followed by the addition of BSA solution for incubation and blocking. After the blocking solution was removed, antibodies were added to the samples dropwise, and finally, the nuclei were stained with DAPI for fluorescence observation.

Statistical analysis

DESeq2 was used for difference analysis, survival and survminer were used for survival analysis, and standardized pretreatment was carried out. The threshold values $p \leq 0.05$, $|\log_2FC| \geq 1$. Enrichment analysis was performed using clusterProfiler, and the threshold was $p < 0.05$.

All the data were analysed with SPSS statistical software 16.0 (SPSS Inc., Chicago, IL, United States) and GraphPad Prism 8 software (GraphPad Software, La Jolla, CA, United States). $P < 0.05$ was considered to indicate a statistically significant difference between values.

Results

Correlation between HRAS expression and prognosis

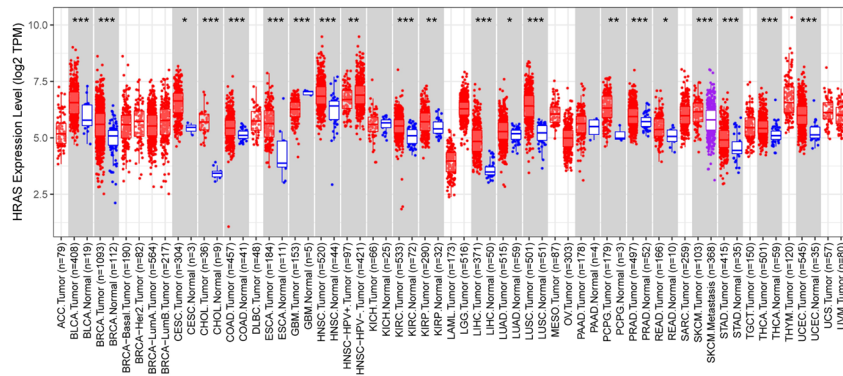
We utilized LIHC data from the TCGA to identify genes that were differentially expressed between normal and tumour tissues. HRAS gene expression was elevated in tumour tissues compared with normal tissues and significantly elevated in LIHC cells (Fig. 2A–C). In addition, by examining the expression of HRAS in the GSE76427, GSE64041, and GSE25097 datasets, we found that the results were the same as those obtained from the TCGA database (Fig. 2D–E) and that HRAS was highly expressed in tumour tissues.

HRAS is a key factor influencing OS

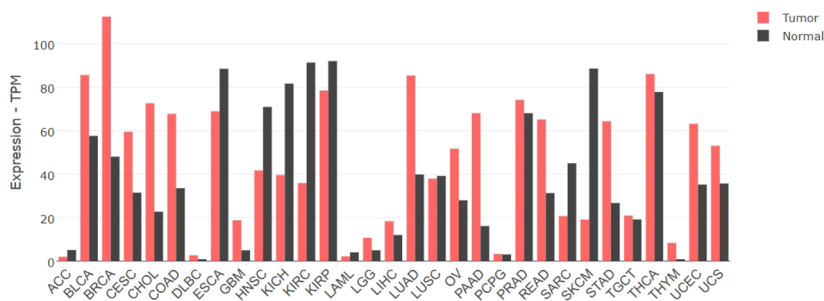
To investigate the relationship between HRAS expression levels and patient OS, we applied Kaplan–Meier curve analysis. The results revealed that patients expressing higher levels of HRAS had a longer OS than patients with lower HRAS expression (Fig. 2G). Thus, HRAS is a key factor influencing OS in LIHC patients.

Relationships between HRAS expression and clinicopathologic features

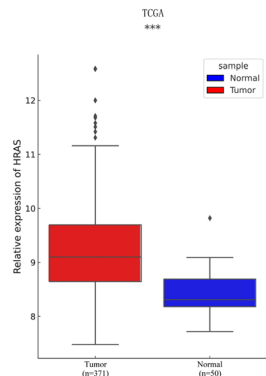
The relationships between the HRAS expression levels and clinicopathological characteristics of patients in the TCGA database were analysed, and the results revealed that higher T stage and pathological stage LIHC patients and female patients had higher HRAS expression levels. In contrast, HRAS expression was



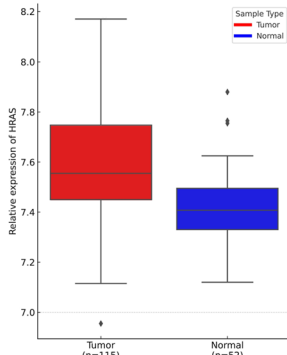
A



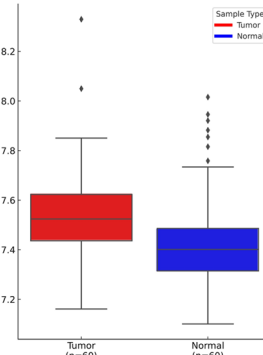
B



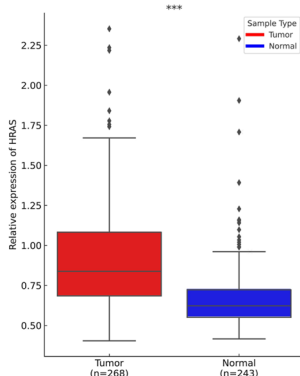
C



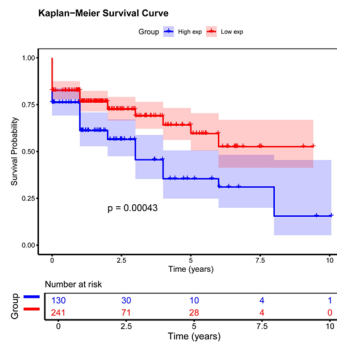
D



E



F



G

Fig. 2 HRAS is highly expressed in tumours and affects OS. **A-C** Compared with normal tissue, HRAS is highly expressed in tumour tissues (normal = 50, tumour = 371). **D** HRAS expression in the GSE76427 dataset (normal = 52, tumour = 115). **E** HRAS expression in the GSE64041 dataset (normal = 60, tumour = 60). **F** HRAS expression in the GSE25097 dataset (normal = 243, tumour = 268). **G** Kaplan–Meier curves of the overall survival of LIHC patients in different clusters

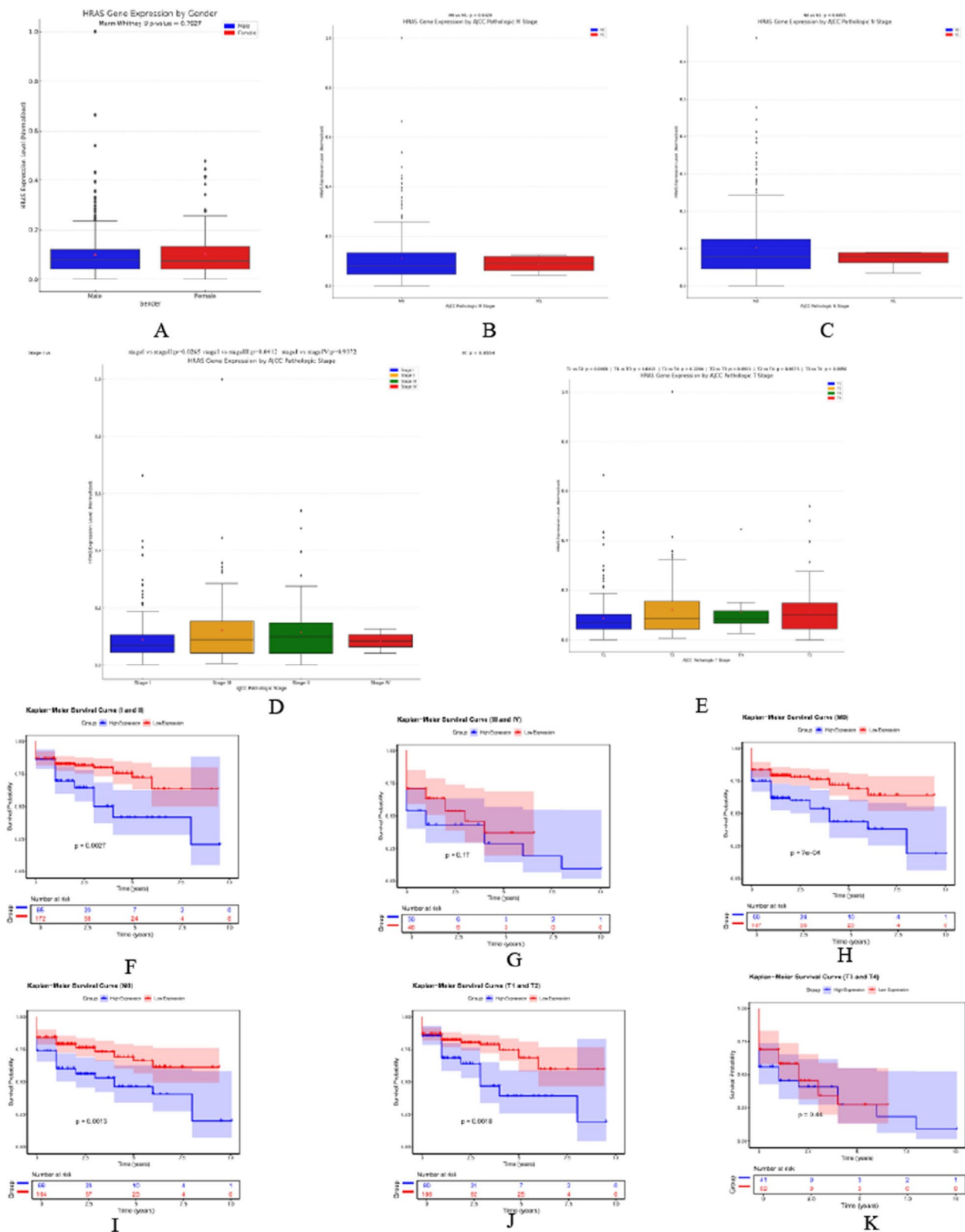
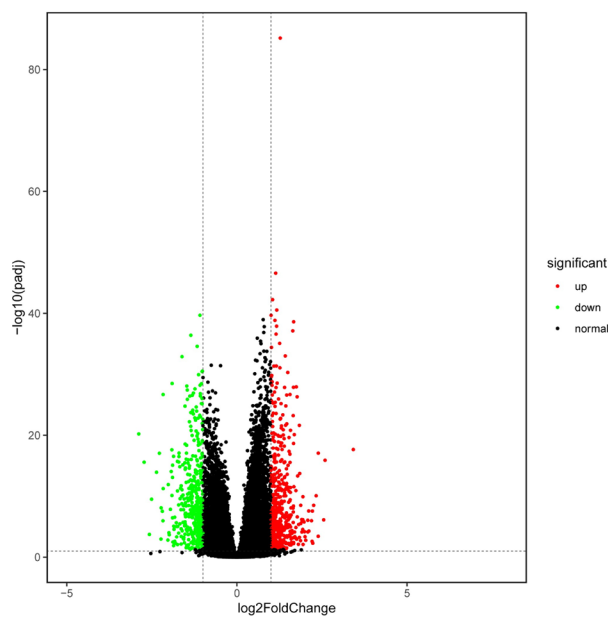


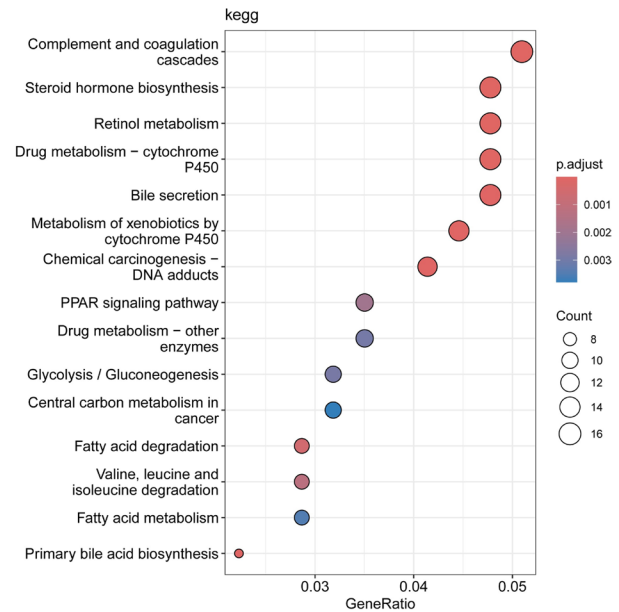
Fig. 3 Relationships between HRAS expression and clinicopathologic features. **A-E** Relationships between HRAS expression and sex and M stage, N stage, overall stage, and T stage tumours. **F-K** Kaplan–Meier curve analyses of phases 1 and 2; 3 and 4; m0 and N0; T1 and T2; and T3 and T4

not associated with sex, pathological stage, N stage, or M stage in patients with LIHC (Fig. 3A-E). Kaplan–Meier curve analysis revealed that HRAS expression was not associated with OS in patients with stage T3 - 4

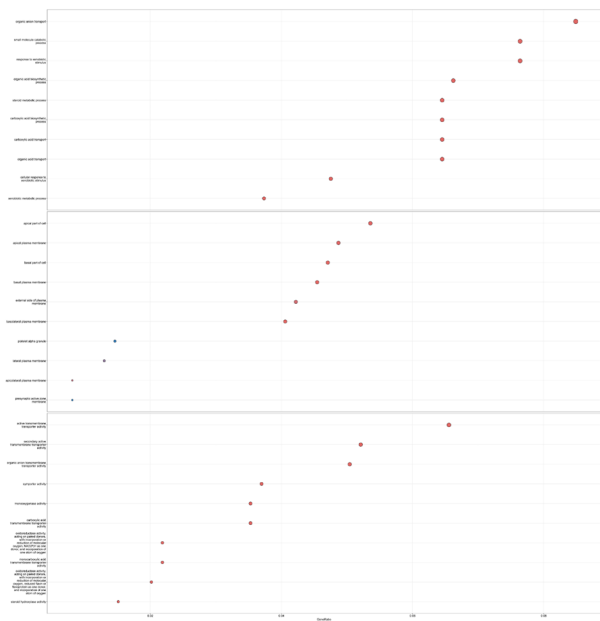
or III-IV LIHC. However, high HRAS expression was associated with poor LIHC prognosis in stage T1 -2, M0, N0, or I-II patients disease (Fig. 3F-K).



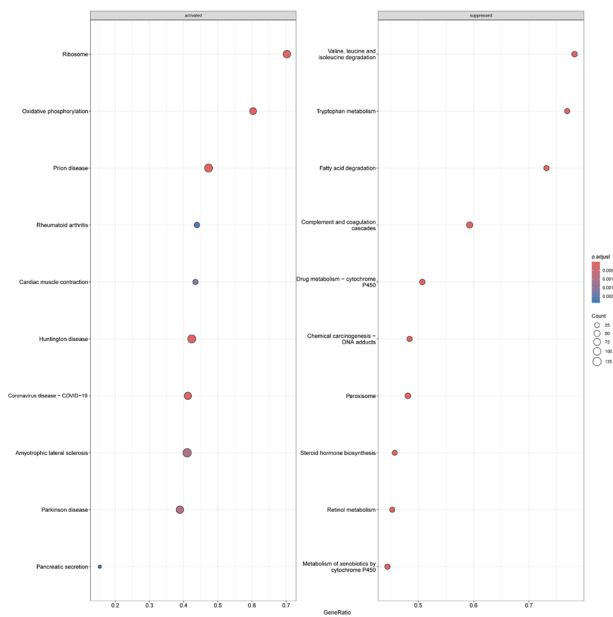
A



B



C



D

Fig. 4 Association between high HRAS expression and poor prognosis. **A** Volcano plot of differentially expressed genes between patients with high and low HRAS expression. **B** KEGG inhibition and activation map. **C** GO enrichment analysis bubble diagram. **D** GSEA inhibition and activation maps

High HRAS expression is associated with poor prognosis

Differences in gene expression between the high- and low-expression subgroups of HRAS tissues were visualized using volcano plots (Fig. 4A). KEGG analysis identified complement and coagulation cascade reactions, central carbon metabolism in cancer, the PPAR signaling pathway, steroid hormone biosynthesis, tyrosine metabolism, and drug metabolism-other enzymes to be associated with abnormally elevated HRAS expression was (Fig. 4B). GO analysis revealed that high HRAS expression was closely related to small molecule catabolic processes, xenobiotic metabolic processes, lipolytic metabolic processes, and vascular transport, among other functions (Fig. 4C). In addition, GSEA revealed that high HRAS expression was closely associated with the activation of pancreatic secretion, oxidative phosphorylation, myocardial contraction via steroid hormone biosynthesis, complement and coagulation cascade reactions, and the inhibition of fatty acid degradation (Fig. 4D).

Correlations between LIHC and immune-related prognostic features

To further investigate the role of prognostic genes in the tumour microenvironment, we analysed data from the TIMER database to study the mechanism of poor prognosis in LIHC patients with elevated HRAS expression. HRAS expression was significantly associated with B cell, CD8 + T cell, CD4 + T cell, macrophage, neutrophil, and dendritic cell infiltration (Fig. 5).

Prognostic model of LIHC

The correlations between all of the genes in the patient sample dataset from the TCGA database and HRAS gene were calculated, and the top ten genes (PSMG3, RPLP2, JPT1, NUDT1, PPP1R14BP3, SURF2, PPP1R14B, NME1, BOLA2B, and POLR2I) were selected for AI classification modelling. Figure 6A-B shows the correlations of these ten genes with the HRAS gene and the expression levels of these ten genes in the patient and normal groups. Before the AI classification model was built, the four datasets (TCGA, GSE76427, GSE64041, and GSE25097) were integrated into a new dataset, and the expression levels of these ten genes and the HRAS gene were extracted from the new dataset for analysis. Next,

we screened the dataset for features using the LASSO algorithm and identified seven genes, SURF2, PSMG3, BOLA2B, PPP1R14B, HRAS, PPP1R14BP3, and JPT1, as the features and then modelled the screened features using the RF, SVM, and KNN machine learning methods. Model fitting established each parameter, as shown in Table 1. Finally, we found that the AI classification model built using LASSO + KNN displayed the best performance, as some of the other models were overfit. Moreover, when seven features, including the HRAS gene, were used, liver cancer tissues were well distinguished from normal tissue samples. Figure 6C-D shows the ROC curves for the training and test datasets.

HRAS promotes LIHC

To verify that HRAS promotes LIHC, we examined the levels of HRAS in HepG2, HepB3, HuH-7 and HL-7702 cells and found that the expression of HRAS was significantly greater in hepatocellular carcinoma cells than in normal hepatocytes (Fig. 7A, C). We subsequently knocked down the HRAS gene to explore its effect on tumour cells. Knockdown of HRAS resulted in decreased cell proliferation, migration and invasiveness (Fig. 7E-G). To further investigate the role of HRAS in tumorigenesis, we examined AKT and PI3K protein expression and concluded that HRAS regulates tumorigenesis through the AKT/P13 K signalling pathway (Fig. 7H).

We injected cancer cells into mice and observed the sizes and weights of the tumours after they formed. The tumour growth rate and size were significantly greater in the LIHC group than in the NC group (Fig. 8A-D). The tumour tissues were subsequently subjected to WB analysis, and high HRAS expression was detected in the tumour tissues (Fig. 8E). HE staining revealed that the cells in the tumour tissues of the LIHC group were tightly arranged and proliferated vigorously (Fig. 8F). Immunohistochemical and immunofluorescence staining revealed a significant increase in HRAS expression in the LIHC group compared with the normal group (Fig. 8G-H). Therefore, the overexpression of HRAS can promote the development of tumours.

To verify the role of HRAS in vivo, we injected tumour cells with HRAS knockdown into nude mice and observed tumour growth. HRAS knockdown tumours

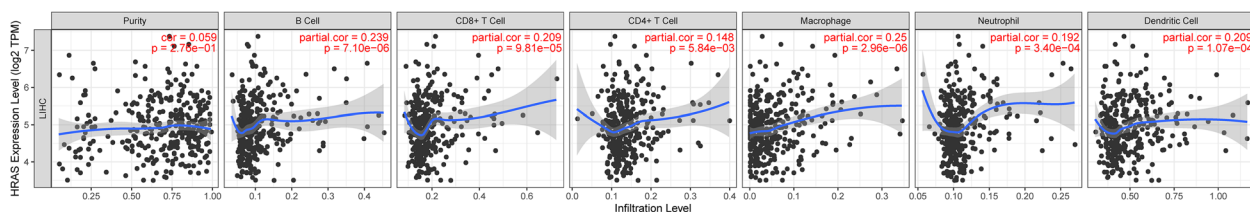


Fig. 5 Associations of HRAS expression with immune cell infiltration

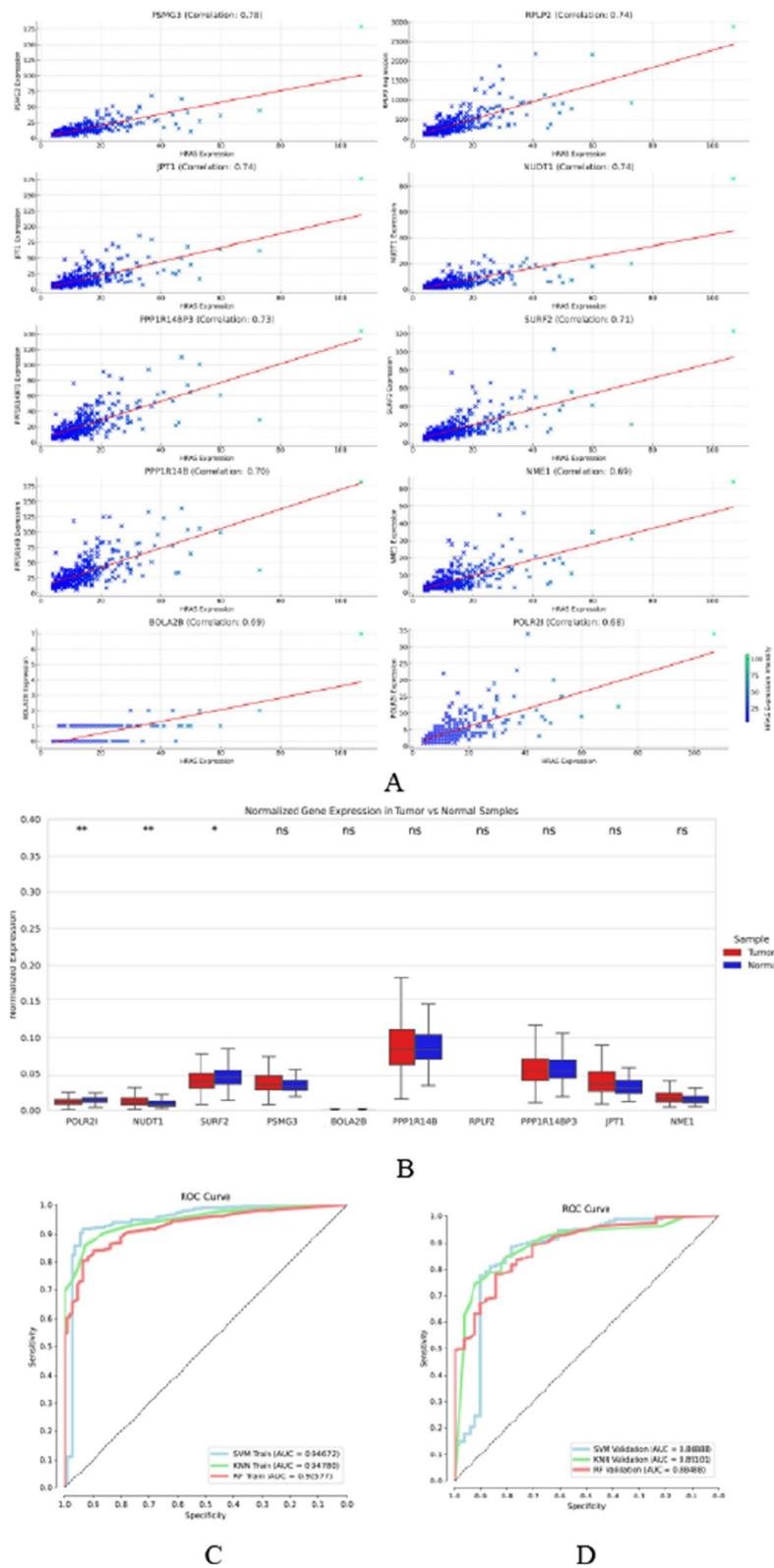


Fig. 6 Prognostic model of LIHC. **A-B** Correlations of ten genes with the HRAS gene and the expression levels of these ten genes in the patient and normal groups. **C-D** ROC curves for the training and test datasets

Table 1 Artificial intelligence model fitting parameters

	Accuracy	Precision	Recall	F1	AUC	Sensitivity
Training set						
SVM	0.899396378	0.924242424	0.948186528	0.936061381	0.946716146	0.948186528
KNN	0.893360161	0.958677686	0.901554404	0.929238985	0.947801428	0.901554404
RF	0.867203219	0.890243902	0.945595855	0.917085427	0.925769033	0.945595855
Test set						
SVM	0.859813084	0.90797546	0.90797546	0.90797546	0.868880067	0.90797546
KNN	0.841121495	0.916129032	0.871165644	0.893081761	0.891014074	0.871165644
RF	0.85046729	0.883040936	0.926380368	0.904191617	0.884879105	0.926380368

were smaller and grew slower (Fig. 9A-E). The HE staining results revealed that knockdown of HRAS resulted in tumours with dispersed cells and decreased density (Fig. 9F). Additionally, immunohistochemical and immunofluorescence staining showed a significant increase in HRAS expression in the LIHC group compared with that in the siNC group. Therefore, the overexpression of HRAS can promote the development of tumours.

In order to further explore the role of HRAS in LIHC, we knocked down HRAS in Hep3B cells, performed HRAS detection (Fig. 10A and C), and observed the cell activity (Fig. 10B). To explore the relationship between HRAS and immune cell infiltration, LIHC cells in which the HRAS gene was knocked down were cocultured with CD4 + T cells, and surface markers of B cells, CD8 + T cells, tumour-associated macrophages, neutrophils, and dendritic cells were detected. As shown in Fig. 10E, the contents of immune cell markers decreased after HRAS knockdown, indicating that HRAS expression was related to immune cell infiltration. In addition, we also believe that HRAS regulates the occurrence of immune infiltration through PI3K/AKT (Fig. 10D). In primary cancer, HRAS expression was detected by IHC (Fig. 10F). This indicated that the level of HRAS expression was positively correlated with the degree of malignancy. In conclusion, HRAS overexpression can promote the occurrence and development of LIHC by regulating the abundance of relevant infiltrating immune cells in the tumour microenvironment.

Discussion

Despite recent advances in adjuvant chemotherapy, molecularly targeted therapies, and immunotherapy, which have improved the outcomes of LIHC patients, long-term patient survival remains poor. Therefore, there is an urgent need to identify more reliable and sensitive prognostic indicators to detect the progression of LIHC and assess patient survival.

In this study, we obtained gene expression data from the TCGA database. Analysis of LIHC-related genes revealed that HRAS was differentially expressed between tumour and normal tissues. Survival and Cox regression analyses revealed the prognostic value of HRAS in LIHC. Surprisingly, patients had poorer outcomes when HRAS was upregulated, which we hypothesized was related to the immune response. Therefore, we used the TIMER database to analyse the relationship between elevated HRAS expression and immune cells. We found that tumour immune cell infiltration was closely associated with high HRAS expression. In addition, fitting the AI classification model built by LASSO + KNN yielded the best results, and the ROC curves and calibration plots confirm the accuracy of prognosis. Finally, we verified the association between HRAS expression and LIHC development through in vivo and in vitro experiments.

RAS proteins are small molecules. In the present study, HRAS was considered a central target in the fight against hepatocellular carcinoma. HRAS is a member of the RAS family that couples extracellular signals to intracellular effector pathways involved in cellular processes [12]. HRAS expression is typically elevated in liver disease and thus an important target for the treatment of liver disease. The administration of an extract of *Artemisia stechmanniana* attenuated liver injury by downregulating HRAS and through the PI3K–AKT pathway [13]. Similarly, Wu's team reported that ginseng Huang jiu improved alcoholic liver disease by modulating HRAS gene expression [14]. In cancer specimens, HRAS promotes CSC production, mainly by activating the RAF/MEK/ERK pathway, to induce SOX2 expression and normal fibroblast reprogramming [15]. The nuclear translocation of SKP2 in human LIHC samples is associated with the activation of the AKT/mTOR and RAS/RAF/MAPK pathways, which promote hepatocellular carcinoma in vivo [16]. An analysis of multiomics data revealed that HRAS affects immune

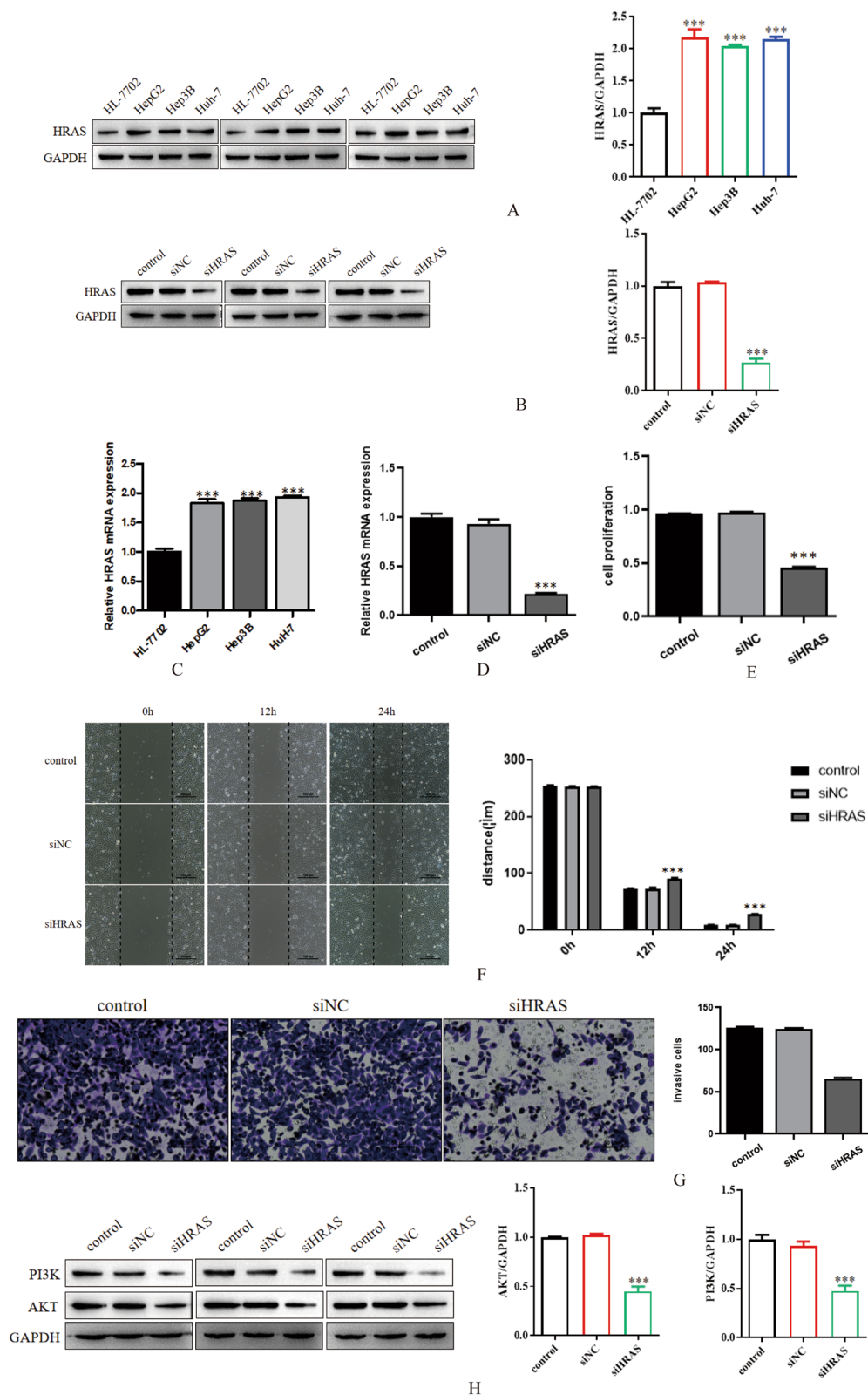


Fig. 7 Investigating the role of HRAS in tumour growth. **A** HRAS expression is elevated in three types of hepatocellular carcinoma cells. **B** Knockdown of HRAS expression after treatment. **C** qRT-PCR detection of HRAS expression in four cell types. **D** qRT-PCR analysis of HRAS expression after knockdown. **E** Cell proliferation decreased after HRAS knockdown. **F** A scratch assay was used to detect cell migration. **G** Cell invasion decreased after HRAS knockdown. **H** HRAS regulates tumour development through the AKT/PI3K pathway

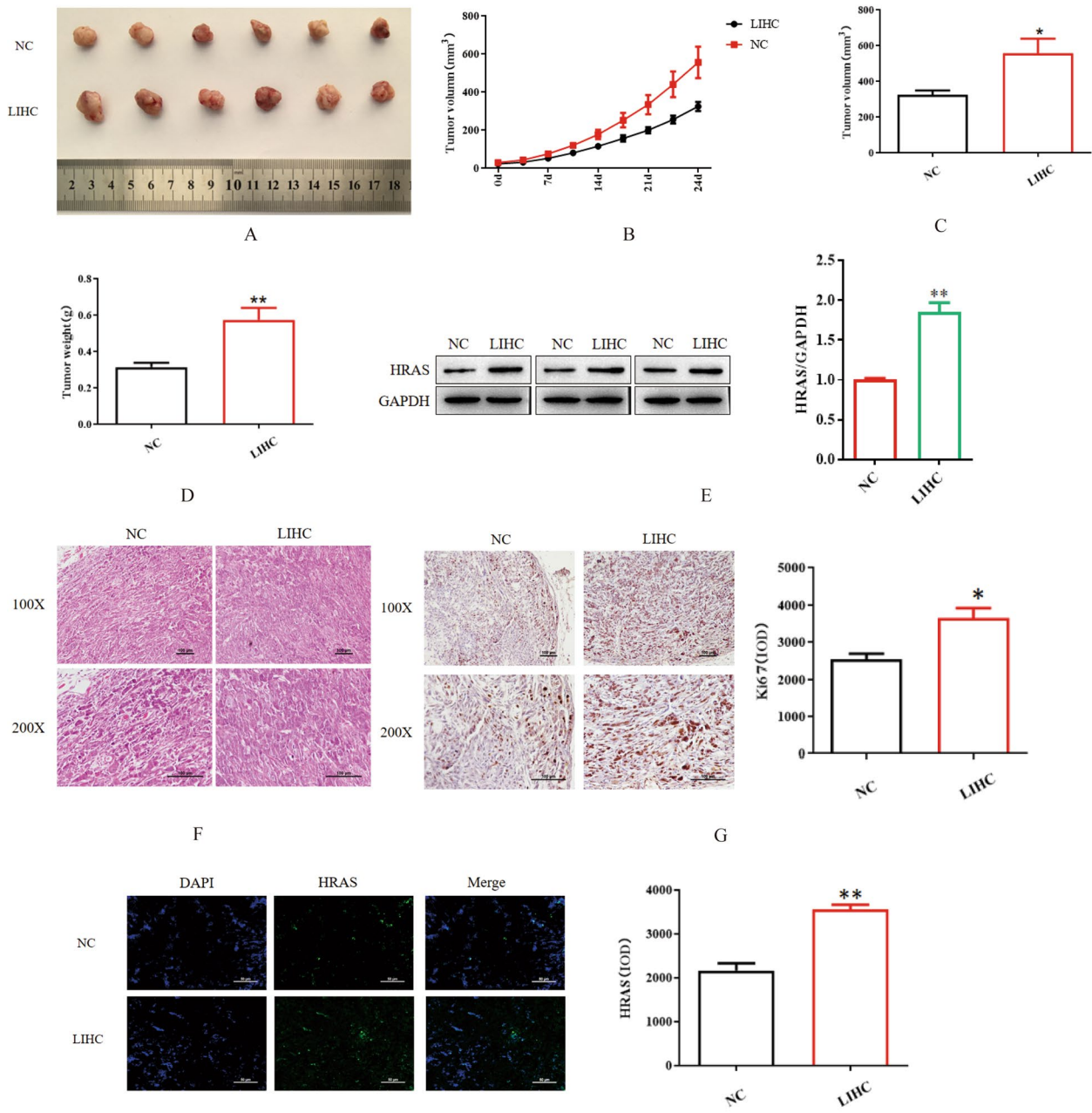


Fig. 8 Investigating the role of HRAS in tumour growth in vivo. **A** Tumour sizes. **B** Tumour growth curves. **C** Tumour volumes. **D** Tumour weights. **E** HRAS expression in mouse tumour tissues. **F** HE staining images of mouse tumour tissues. **G** IHC staining of HRAS in tumour sections. **H** IHC staining of HRAS in tumour sections

cell infiltration, which is correlated with iron-mediated cell death and more directly predicts the probability of survival in patients with LIHC [17]. In our study, HRAS expression was strongly associated with poor LIHC prognosis.

In the context of cancer, cells in the tumour micro-environment contribute to cancer cell proliferation,

immunosuppression and angiogenesis to support tumour growth and metastasis. This study revealed that HRAS affects the prognosis of LIHC mainly by regulating immune cell infiltration. In previous studies, an increased abundance of B cells was associated with poor hepatocellular carcinoma prognosis [18]. A previous study revealed that increased CD4 + T-cell

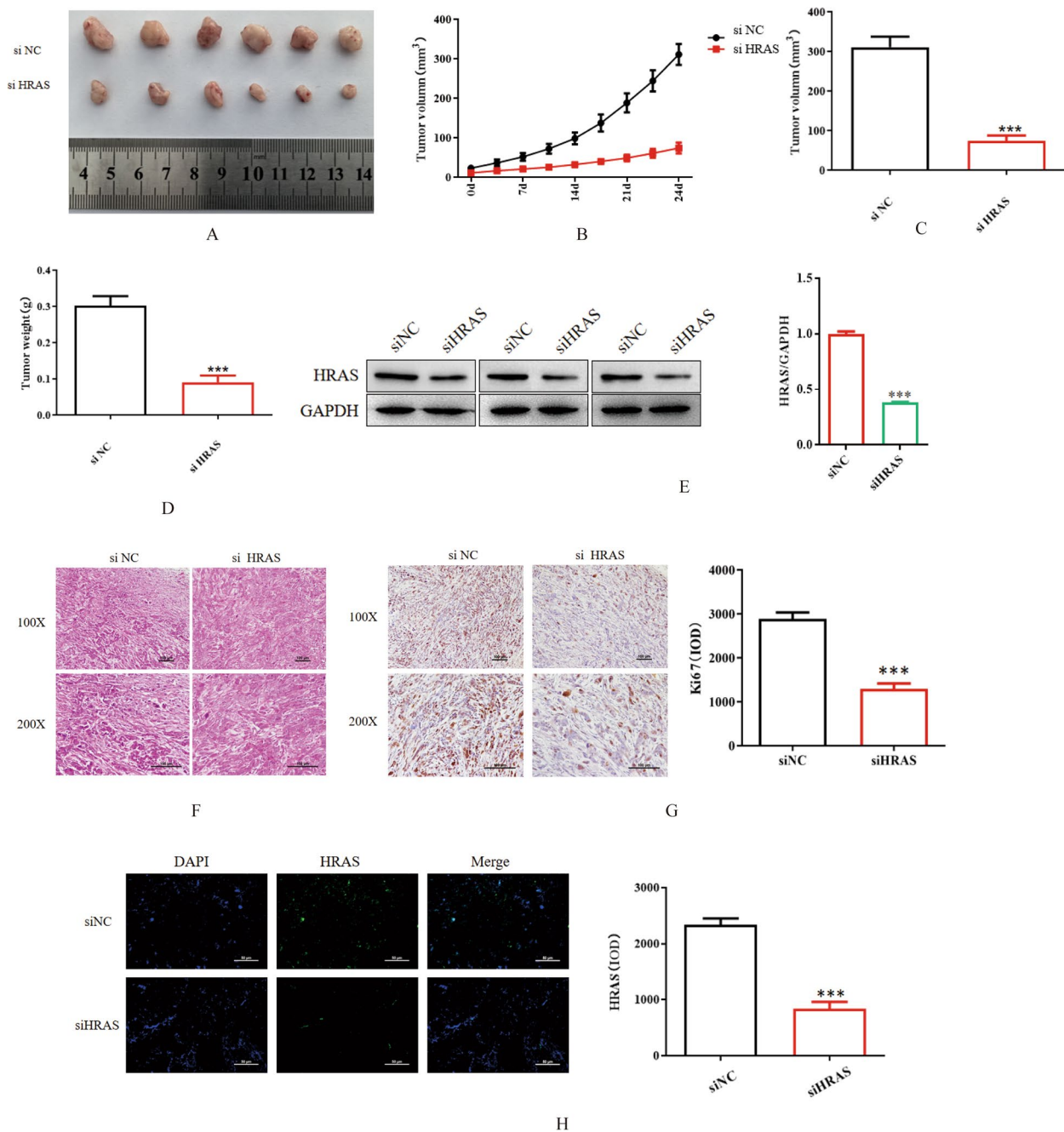


Fig. 9 Tumour growth in vivo after HRAS knockdown. **A** Knockdown of HRAS results in smaller tumours. **B** Tumour growth curves. **C** Tumour volumes after HRAS knockdown. **D** Tumour volumes after HRAS knockdown. **E** HRAS expression in mouse tumour tissues. **F** HE staining images of mouse tumour tissues. **G** IHC staining of HRAS in tumour sections. **H** IF staining of HRAS in tumour sections

infiltration occurs at the tumour site [19]. CD4 + T cells and NK cells synergize more strongly than CD8 + cells and NK cells do in tumour immunotherapy approaches [20]. In addition, Maestri’s team biopsied LIHC patients and concluded that CD8 + T cells in close proximity to tumours was a favourable predictor of patient

outcomes [21]. Clinically, the presence of macrophages within primary tumours has been shown to be correlated with poorer prognosis in almost all tumour types [22]. Zhang et al. constructed a prognostic model for LIHC on the basis of macrophages, revealing that macrophage infiltration was significantly greater in LIHC

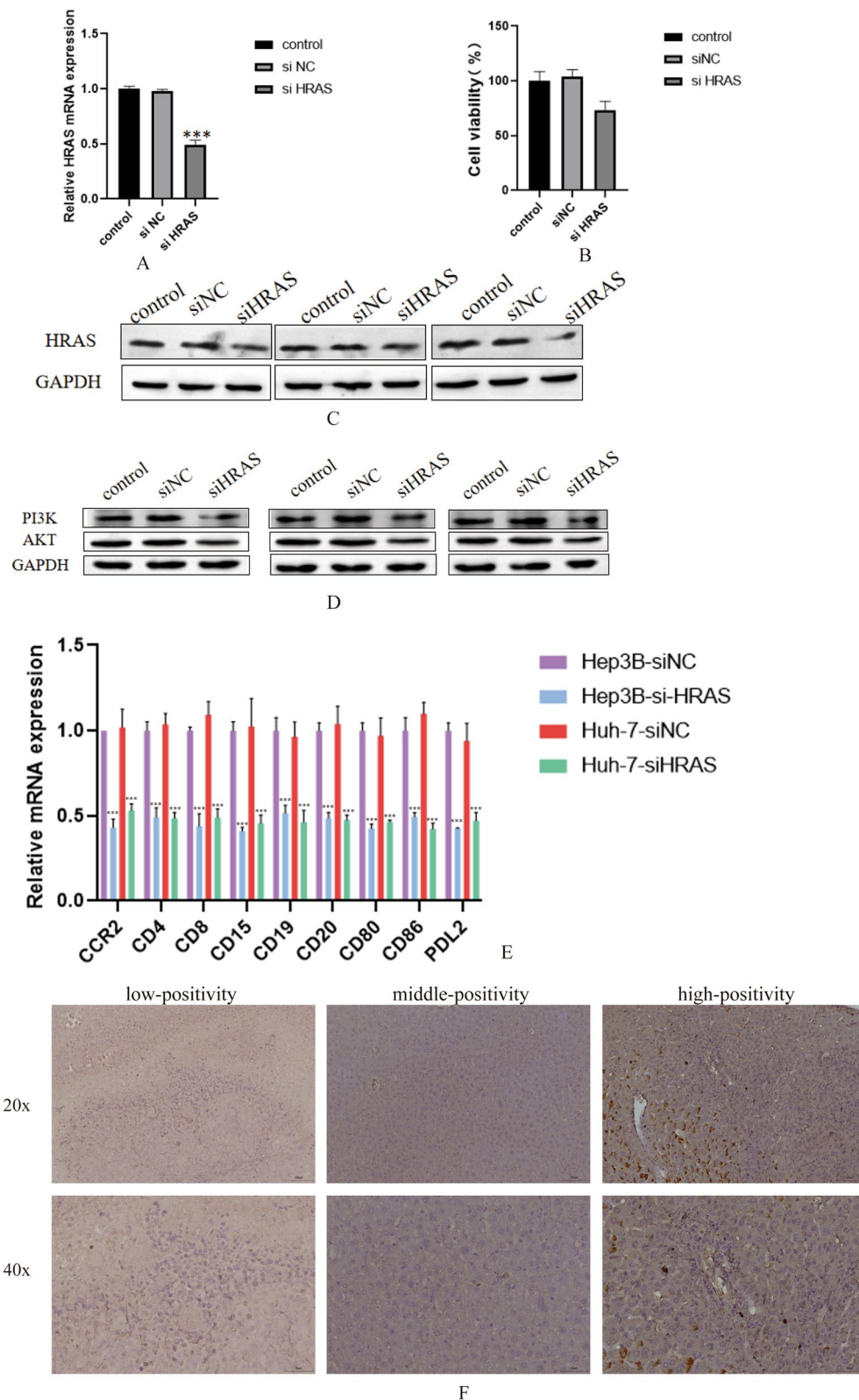


Fig. 10 HRAS and immune correlation in LIHC. **A** Knockdown of HRAS expression in Hep3B cells. **B** Reduced cell activity after knockdown of HRAS in Hep3B cells. **C** Detection of HRAS expression in cells by WB. **D** HRAS regulates tumour development through the PI3K/AKT pathway. **E** Marker molecules associated with immune infiltration decreased after knockdown of HRAS. **F** HRAS expression in primary cancers by IHC

tissues than in normal liver tissues [23]. Furthermore, in Liu's study, HRAS was found to be involved in LIHC prognosis and correlated with the tumour immune processes [24]. Wang et al. screened immune genes closely related to prognosis by analysing the immune gene profiles of Asians with LIHC and reported that HRAS plays a role in signalling pathways and has a significant effect on the survival of LIHC patients [25]. HRAS expression is positively correlated with the infiltration of M2 macrophages and activated NK cells in LIHC tumours and can be used to predict patient survival and tumour immunity [26]. This finding is consistent with our findings, and may be the reason why high HRAS expression indicated a poor prognosis in our study.

Conclusion

In conclusion, we identified and validated HRAS as a biomarker related to immunity in LIHC patients. Here, we show its robust performance in predicting the prognosis and infiltration of immune cells in LIHC. Furthermore, our study analysed the factors associated with poor LIHC prognosis and lays a foundation for future developments. These data indicate that HRAS expression may be useful in determining LIHC prognosis.

Abbreviations

LIHC	Liver hepatocellular carcinoma
TCGA	The Cancer Genome Atlas
HRAS	HRas proto-oncogene, GTPase
KEGG	Kyoto Encyclopedia of Genes and Genomes
GO	Gene Ontology
GSEA	Gene set enrichment analysis

Supplementary Information

The online version contains supplementary material available at <https://doi.org/10.1186/s12885-025-14131-x>.

Supplementary Material 1.

Acknowledgements

We thank Kunming Medical University for providing experimental guidance, and Springer for providing language services.

Authors' contributions

A and B: writing, modifying, cellular functions, study of molecular mechanisms. C: Experimental cell research. D: Animal experimental research. E: Clinical level research. F: Revision of articles. G: Revision of article. H and I: Overall design and direction of the dissertation. All authors reviewed the manuscript.

Funding

This work was supported by funds from the Yunnan Provincial Department of Science and Technology Basic Research Program, Kunming Medical Joint Special General Project (202401AY070001-260) and the Key Projects of Faculty Research Programs of The First People's Hospital of Qujing City (2022YJKZ01).

Data availability

The database used in this study was obtained from the TCGA database (<https://portal.gdc.cancer.gov/>).

Declarations

Ethics approval and consent to participate

The human database used in this study follows the Declaration of Helsinki. All methods were carried out in accordance with relevant guidelines and regulations. The animal experimental methods were reported in accordance with ARRIVE guidelines (<https://arriveguidelines.org>) and were approved by Kunming Medical University Affiliated Qujing Hospital (Qujing, China).

Consent for publication

Not applicable.

Competing interests

The authors declare no competing interests.

Author details

¹Hepatobiliary Pancreatic Surgery, Kunming Medical University Affiliated Qujing Hospital (The First People's Hospital of Qujing City, Yunnan Province), Qujing, Yunnan Province 655000, China. ²Pathology Teaching and Research Office, Qujing Medical College, Qujing, Yunnan Province 655000, China.

Received: 21 October 2024 Accepted: 10 April 2025

Published online: 28 April 2025

References

- Llovet JM, Kelley RK, Villanueva A, et al. Hepatocellular carcinoma. *Nat Rev Dis Primer.* 2021;7(1):6. <https://doi.org/10.1038/s41572-020-00240-3>.
- Anwanwan D, Singh SK, Singh S, Saikam V, Singh R. Challenges in liver cancer and possible treatment approaches. *Biochim Biophys Acta Rev Cancer.* 2020;1873(1):188314. <https://doi.org/10.1016/j.bbcan.2019.188314>.
- Chen L, Wei X, Gu D, Xu Y, Zhou H. Human liver cancer organoids: biological applications, current challenges, and prospects in hepatoma therapy. *Cancer Lett.* 2023;555:216048. <https://doi.org/10.1016/j.canlet.2022.216048>.
- Lim JKM, Leprivier G. The impact of oncogenic RAS on redox balance and implications for cancer development. *Cell Death Dis.* 2019;10(12):955. <https://doi.org/10.1038/s41419-019-2192-y>.
- Jagadeeshan S, Prasad M, Badarni M, et al. Mutated HRAS activates YAP1-AXL signaling to drive metastasis of head and neck cancer. *Cancer Res.* 2023;83(7):1031–47. <https://doi.org/10.1158/0008-5472.CAN-22-2586>.
- Li S, Wu L, Zhang H, et al. GINS1 induced sorafenib resistance by promoting cancer stem properties in human hepatocellular cancer cells. *Front Cell Dev Biol.* 2021;9:711894. <https://doi.org/10.3389/fcell.2021.711894>.
- Ling C, Liu SS, Wang YY, et al. Overexpression of wild-type HRAS drives non-alcoholic steatohepatitis to hepatocellular carcinoma in mice. *Zool Res.* 2024;45(3):551–66. <https://doi.org/10.24272/j.jissn.2095-8137.2024.002>.
- Ye Y, Zhang S, Jiang Y, et al. Identification of a cancer associated fibroblasts-related index to predict prognosis and immune landscape in ovarian cancer. *Sci Rep.* 2023;13(1):21565. <https://doi.org/10.1038/s41598-023-48653-w>.
- Tran Janco JM, Lamichhane P, Karyampudi L, Knutson KL. Tumor-infiltrating dendritic cells in cancer pathogenesis. *J Immunol.* 2015;194(7):2985–91. <https://doi.org/10.4049/jimmunol.1403134>.
- Dakal TC, George N, Xu C, Suravajhala P, Kumar A. Predictive and prognostic relevance of tumor-infiltrating immune cells: tailoring personalized treatments against different cancer types. *Cancers.* 2024;16(9):1626. <https://doi.org/10.3390/cancers16091626>.
- Gui Z, Ye Y, Li Y, et al. Construction of a novel cancer-associated fibroblast-related signature to predict clinical outcome and immune response in cervical cancer. *Transl Oncol.* 2024;46:102001. <https://doi.org/10.1016/j.tranon.2024.102001>.
- Pylayeva-Gupta Y, Grabocka E, Bar-Sagi D. RAS oncogenes: weaving a tumorigenic web. *Nat Rev Cancer.* 2011;11(11):761–74. <https://doi.org/10.1038/nrc3106>.

13. Tian CB, Qin ML, Qian YL, et al. Liver injury protection of *Artemisia stechmanniana* better through PI3K/AKT pathway. *J Ethnopharmacol*. 2024;334:118590. <https://doi.org/10.1016/j.jep.2024.118590>.
14. Wu Y, Cai Y, Ma L, et al. Identification and chemical profiling of anti-alcoholic liver disease biomarkers of ginseng Huang jiu using UPLC-Q-Orbitrap-HRMS and network pharmacology-based analyses. *Front Nutr*. 2022;9:978122. <https://doi.org/10.3389/fnut.2022.978122>.
15. Shimizu M, Shibuya H, Tanaka N. Enhanced O-GlcNAc modification induced by the RAS/MAPK/CDK1 pathway is required for SOX2 protein expression and generation of cancer stem cells. *Sci Rep*. 2022;12(1):2910. <https://doi.org/10.1038/s41598-022-06916-y>.
16. Delogu S, Wang C, Cigliano A, et al. SKP2 cooperates with N-Ras or AKT to induce liver tumor development in mice. *Oncotarget*. 2015;6(4):2222–34. <https://doi.org/10.18632/oncotarget.2945>.
17. Zhang L, Chen X, Guo X, et al. Comprehensive analysis of cell death genes in hepatocellular carcinoma based on multi-omics data. *Adv Clin Exp Med Off Organ Wroclaw Med Univ*. 2023;32(2):233–44. <https://doi.org/10.17219/acem/152737>.
18. Yin L, Chen L, Qi Z, et al. Gene expression-based immune infiltration analyses of liver cancer and their associations with survival outcomes. *Cancer Genet*. 2021;254–255:75–81. <https://doi.org/10.1016/j.cancergen.2021.02.001>.
19. Rohr-Udilova N, Klingmüller F, Schulte-Hermann R, et al. Deviations of the immune cell landscape between healthy liver and hepatocellular carcinoma. *Sci Rep*. 2018;8(1):6220. <https://doi.org/10.1038/s41598-018-24437-5>.
20. Perez-Diez A, Joncker NT, Choi K, et al. CD4 cells can be more efficient at tumor rejection than CD8 cells. *Blood*. 2007;109(12):5346–54. <https://doi.org/10.1182/blood-2006-10-051318>.
21. Maestri E, Kedei N, Khatib S, et al. Spatial proximity of tumor-immune interactions predicts patient outcome in hepatocellular carcinoma. *Hepatol Baltim Md*. 2024;79(4):768–79. <https://doi.org/10.1097/HEP.0000000000000600>.
22. Ngambenjawong C, Gustafson HH, Pun SH. Progress in tumor-associated macrophage (TAM)-targeted therapeutics. *Adv Drug Deliv Rev*. 2017;114:206–21. <https://doi.org/10.1016/j.addr.2017.04.010>.
23. Zhang Y, Zou J, Chen R. An M0 macrophage-related prognostic model for hepatocellular carcinoma. *BMC Cancer*. 2022;22(1):791. <https://doi.org/10.1186/s12885-022-09872-y>.
24. Liu Z, Yang L, Liu C, et al. Identification and validation of immune-related gene signature models for predicting prognosis and immunotherapy response in hepatocellular carcinoma. *Front Immunol*. 2024;15:1371829. <https://doi.org/10.3389/fimmu.2024.1371829>.
25. Wang Y, Feng Z, Zhang Y, Zhang Y. Establishment and verification of a prognostic risk score model based on immune genes for hepatocellular carcinoma in an Asian population. *Transl Cancer Res*. 2023;12(10):2806–22. <https://doi.org/10.21037/tcr-23-128>.
26. Zou J, Qin W. Comprehensive analysis of the cancer driver genes constructs a seven-gene signature for prediction of survival and tumor immunity in hepatocellular carcinoma. *Front Genet*. 2022;13:937948. <https://doi.org/10.3389/fgene.2022.937948>.

Publisher's Note

Springer Nature remains neutral with regard to jurisdictional claims in published maps and institutional affiliations.